Nonlinear Dyn (2015) 81:577–583
DOI 10.1007/s11071-015-2012-6

ORIGINAL PAPER

# On two-parameter bifurcation analysis of the periodic parameter-switching Lorenz oscillator

**Chun Zhang · Qinsheng Bi**

Received: 13 June 2014 / Accepted: 4 March 2015 / Published online: 19 March 2015


**Abstract** By introducing the periodic parameter-switching scheme to the Lorenz oscillator, a switched dynamic model is established. In order to investigate the mechanism of the behaviors of the switched system, the Poincaré map of the whole system is defined by suitable local sections and local maps. Different types of periodic oscillations and their transitions to chaos in the system can be observed. Based on the conditions when the Floquet multiplies of corresponding fixed point associated with the periodic solution pass the unit circle, some bifurcation curves are obtained in the plane of bifurcation parameters, dividing the parameters plane into several regions corresponding to different kinds of oscillations. Meanwhile, bifurcation scenarios, such as fold bifurcation, pitchfork bifurcation and period-doubling bifurcation, are determined in the switched system.

**Keywords** Switched system · Poincaré map · Floquet multiplies · Bifurcation mechanism

C. Zhang (✉)
School of Mathematical Science, Huaiyin Normal University, Huai'an 223300, Jiangsu, People's Republic of China
e-mail: zhchun1984@yahoo.cn

Q. Bi
Faculty of Science, Jiangsu University, Zhenjiang 212013, Jiangsu, People's Republic of China
e-mail: qinbi1968@163.com

## 1 Introduction

Among the numerous chaotic systems, the Lorenz model [1], expressed as,

$$\dot{x} = \alpha(y - x),\ \dot{y} = x(\delta - z) - y,\ \dot{z} = xy - \beta z, \quad (1.1)$$

with $\alpha, \beta, \delta > 0$, is the most classical and paradigmatic chaotic system due to a historical reason that it was the first model of chaotic behavior. This simple nonlinear model has received much interest, and a lot of results have been reported [2–4]. It is found that three equilibria, two of which are symmetric with the transformation $(x, y, z) \longrightarrow (-x, -y, z)$, may exist in the system and the trajectory of the system cycling around two symmetric foci may form a chaotic attractor, namely the famous butterfly effect [5]. However, from a practical design point of view, many more chaotic systems with the simpler structures were established, such as Chua's circuit [6], Chen system [7], Lü system [8] and the Lorenz system family [9].

How to control these systems to meet the need, such as to stabilize the oscillations or to control chaos including eliminating or utilizing chaos, is theoretically a very attractive yet technically quite challenging task in nonlinear dynamics [10,11]. For the Lorenz system, many controllers were designed with multiple control inputs or state variable feedbacks [12–17]. In Ref. [12], a simple feedback controller to reduce and even eliminate the chaotic behavior in a controlled Lorenz was investigated. In Refs. [13] and [14], two hyperchaotic Lorenz systems by adding extra variables into Lorenz

system were constructed and the evolution processes of the system were analyzed. In Refs. [15] and [16], a hyperchaotic Lorenz system with the structure of two time scales was constructed and the bursting phenomena as well as the associated bifurcation mechanisms were presented. In Ref. [17], a Lorenz system involving complex variables was established and the differences between the behavioral features of the Lorenz system with complex variables and the Lorenz system with real variables were described. In contrast, in this paper, we consider the scheme that is to use a time-varying, or more preciously, periodically switching parameter associated with the Lorenz oscillator to study the dynamics of the switched Lorenz oscillator.

Generally, switching from one subsystem to another often occurs on a set of borders associated with certain critical state variable or related to a fixed time for the occurrence of alteration [18,19]. When the trajectory crosses the borders, the system is redefined, which means the dynamics may alternate between different types of oscillations determined by subsystems, causing non-smooth phenomena at the switching points. It is noted that the switching may obviously lead to complicated behaviors. However, to our knowledge, little research work related to the switched Lorenz system has been reported [20]. Many problems for the switched systems such as the dynamical evolution with the variation of the parameters and the bifurcations associated with the switches as well as the mechanism of complexity still need further research.

In the following sections, first, the two Lorenz systems that switches between each other based on the parameters altered periodically are described, and then the analyzed methods for symmetric and asymmetric periodic switching oscillators as well as related bifurcation mechanism are explained. Subsequently, the two-parameter bifurcation sets of the switched system and the mechanisms of several typical dynamical behaviors are presented.

## 2 The model of switched system

Let us consider the time switched system

$$\frac{\mathrm{d}\mathbb{X}}{\mathrm{d}t} = f_1(\mathbb{X}, \lambda_1) I_B(t) + f_2(\mathbb{X}, \lambda_2) I_{B^c}(t), \tag{2.1}$$

where

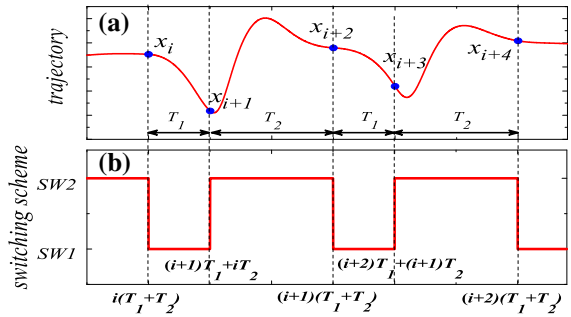


**Fig. 1** **a** Trajectory partition; **b** the switching scheme

$$I_B(t) = \begin{cases} 1, & t \in B, \\ 0, & t \in \mathrm{B}^c, \end{cases} \qquad B = \bigcup_{i=0}^{\infty} \Big[ i(T_1 + T_2), (i+1)T_1 + iT_2 \Big],$$

and $\mathbb{X} = (x, y, z)^T$ are dynamic state. $\lambda_1, \lambda_2 \in \mathbb{R}^r$ are the parameter depending on $f_1$ and $f_2$, respectively. $r$ is integer. $B^c$ is the complementary set of the set $B$. $f_k$ is the vector field with $f_k = (\alpha(y-x), x(\delta_k - z) - y, xy - \beta_k z)^T, k \in \{1, 2\}$. When $t \in B$, subsystem $\dot{\mathbb{X}} = f_1(\mathbb{X}, \lambda_1)$, named SW1, is active, when $t \in B^c$ subsystem $\dot{\mathbb{X}} = f_2(\mathbb{X}, \lambda_2)$, named SW2, is active. Thus, a trajectory of the switched system (2.1) can be partitioned, as depicted for a particular case in Fig. 1a, based on the switching scheme described in Fig. 1b.

Given an initial point $\mathbb{X}_0$, the switched system is governed by SW1. After a period of time $T_1$, SW2 is activated for another relative fixed period of time, $T_2$, which implies that at $t = T_1 + T_2$, the switched system may turn back to SW1 until the next $T_1$ is satisfied and the motion then continues as above. Therefore, the trajectory of switched system can be divided into two parts, one is governed by SW1, expressed as

$$\mathbb{X}(t) = \Phi(t, \mathbb{X}_{2i}, \alpha, \beta_1, \delta_1), \quad t \in B, \tag{2.2}$$

the other is determined by SW2, i.e.,

$$\mathbb{X}(t) = \Psi(t, \mathbb{X}_{2i+1}, \alpha, \beta_2, \delta_2), \quad t \in B^c, \tag{2.3}$$

where $\mathbb{X}_{2i}, \mathbb{X}_{2i+1}$, $i = 0, 1, 2 \ldots$ are the starting points of the two subsystems, respectively.

## 3 Analyzed method

Since the system (2.1) is a time switched system, two switching hyperplanes are conveniently given by (see Fig. 2)

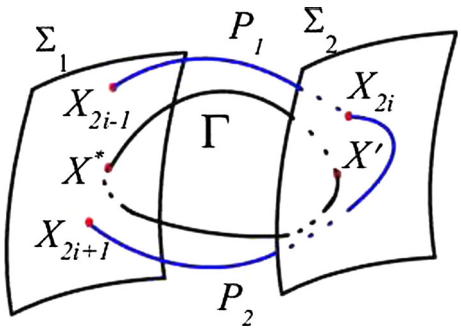


**Fig. 2** Local hyperplanes and local mappings

$$\sum\nolimits_1 = \bigcup_{i=0}^{\infty} \left\{ (\mathbb{X}, t) \in R^3 \times R^+ \mid t = (i+1)T_1 + iT_2 \right\},$$
$$\sum\nolimits_2 = \bigcup_{i=0}^{\infty} \left\{ (\mathbb{X}, t) \in R^2 \times R^+ \mid t = (i+1)(T_1 + T_2) \right\}. \tag{3.1}$$

According to the switching scheme and the definition of the solution of (2.1), points $\{\mathbb{X}_{2i+1}, i = 0, 1, 2, \ldots\}$ are on the hyperplane $\sum_1$, while points $\{\mathbb{X}_{2i}, i = 1, 2, \ldots\}$ are on the hyperplane $\sum_2$. Meanwhile, on the hyperplanes, two local mappings are conveniently defined as (see Fig. 2)

$$\begin{aligned} P_1 &: \sum_1 \longrightarrow \sum_2 : \mathbb{X}_{2i-1} \longmapsto \mathbb{X}_{2i} \\ &= \Psi(T_2, \mathbb{X}_{2i-1}, \alpha, \beta_2, \delta_2), \\ P_2 &: \sum_2 \longrightarrow \sum_1 : \mathbb{X}_{2i} \longmapsto \mathbb{X}_{2i+1} \\ &= \Phi(T_1, \mathbb{X}_{2i}, \alpha, \beta_1, \delta_1). \end{aligned} \tag{3.2}$$

where $i = 1, 2, \ldots$. Thus, the periodic behavior of limit cycle (labeled $\Gamma$ in Fig. 2) of the switched system (2.1) can be expressed as follow

$$\begin{cases} \Psi(T_2, \mathbb{X}^*, \alpha, \beta_2, \delta_2) - \mathbb{X}' = 0, \\ \Phi(T_1, \mathbb{X}', \alpha, \beta_1, \delta_1) - \mathbb{X}^* = 0, \end{cases} \tag{3.3}$$

where the point $\mathbb{X}'$ is on the hyperplane $\sum_2$. Assume that the hyperplane $\sum_1$ is the Poincaré section, the Poincaré mapping $P$ from $\sum_1$ to $\sum_1$ can be expressed as

$$P(\mathbb{X}_{2i-1}) = \Phi\left(T_1, \Psi\left(T_2, \mathbb{X}_{2i-1}, \alpha, \beta_2, \delta_2\right), \alpha, \beta_2, \delta_2\right). \tag{3.4}$$

Essentially, the periodic solution of the switched system (2.1) is equivalent to the existence of the fixed point of the Poincaré mapping $P$, namely

$$\mathbb{X}^* - P(\mathbb{X}^*) = 0. \tag{3.5}$$

The fixed point $\mathbb{X}^*$ is corresponding to the periodic solution of the switched system (2.1) with period $T = T_1 + T_2$, which is called period 1 solution. Similarly, if $\mathbb{X}^* = P^k(\mathbb{X}^*)$ and $\mathbb{X}^* \neq P^m(\mathbb{X}^*), m = 1, 2, \ldots, k-1$, the switched system (2.1) has a period $k$ solution.

Since the subsystems of the switched system (2.1) is invariant with respect to the transformation $\Pi : (x, y, z)^T \mapsto (-x, -y, z)^T$, the solutions of the switched system (2.1) may reflect certain spatial invariance. Assuming matrix $R$ is the transformation matrix corresponding to this transformation, a simple classification of the solutions of the system can be defined.

**(i)** A solution $\Gamma$ of the switched system (2.1) is called symmetric if $R(\Gamma) = \Gamma$.

**(ii)** Two solutions $\Gamma_1, \Gamma_2$ of the switched system (2.1) are called R-conjugate if they satisfy $\Gamma_2 = R(\Gamma_1)$.

The symmetric limit cycles can be located by solving the following equation

$$F(\mathbb{X}^*) := R\big(P(\mathbb{X}^*)\big) - P\big(R(\mathbb{X}^*)\big) = 0. \tag{3.6}$$

The solution $\mathbb{X}^*$ can be obtained using a multiple-shooting method [21], which solves the iterative scheme

$$\mathbb{X}^{k+1} = \mathbb{X}^k - \big(DF(\mathbb{X}^k)\big)^{-1} F\big(\mathbb{X}^k\big), \tag{3.7}$$

where

$$DF(\mathbb{X}^k) = R\big(DP(\mathbb{X}^k)\big) - DP\big(R(\mathbb{X}^k)\big). \tag{3.8}$$

From (3.4), it follows that

$$DP = D\Phi \circ D\Psi. \tag{3.9}$$

The Jacobian matrix $D\Psi$, $D\Phi$ can be computed by the following variational equations

$$\frac{\mathrm{d}}{\mathrm{d}t}(D\Psi) = f_{1\mathbb{X}}(t) D\Psi, \tag{3.10}$$
$$\frac{\mathrm{d}}{\mathrm{d}t}(D\Phi) = f_{2\mathbb{X}}(t) D\Phi, \tag{3.11}$$

with the initial condition $D\Psi|_{t=0} = I$, $D\Phi|_{t=T_1} = I$, respectively. Where $f_{1\mathbb{X}}$, $f_{2\mathbb{X}}$ are the Jacobian matrices of $f_1$, $f_2$. $I$ is an identity matrix. Note that $f_{1\mathbb{X}}$, $f_{2\mathbb{X}}$ are evaluated along the trajectory, and hence are time-varying matrices. Therefore the symmetric periodic

solution of the system (2.1) can be obtained, the stability and the corresponding bifurcations of which can be determined by the associated characteristic equation, written in the form

$$\det(DP - \mu I) = 0, \tag{3.12}$$

where $\mu = (\mu_1, \mu_2, \mu_3)$ is the eigenvalue. For the periodic solution of the switched system, period-doubling bifurcation may occur when $\mu_1 = -1$, while fold or pitchfork bifurcation may take place once $\mu_1 = 1$ (see Ref. [21], Theorem 7.9 and Ref. [22]). Meanwhile, the Lyapunov exponent $\lambda = (\lambda_1, \lambda_2, \lambda_3)$ can be calculated by

$$\lambda = \lim_{N\to\infty} \frac{1}{N} \sum_{k=0}^{N-1} \log|DP(\mathbb{X}_k)| \tag{3.13}$$

where $\mathbb{X}_k = P^k(\mathbb{X}_0)$ (see Ref. [23]). For stable cycles, $\lambda_i, i = 1, 2, 3$ are all negative; for chaotic attractors, there is a Lyapunov exponent $\lambda_i$ which is positive.

## 4 Bifurcations of cycles

In this section, we analyze the bifurcation of the symmetric periodic solution changing the parameters $\beta_2$ and $\delta_2$ and fixing the parameters $\alpha = 5.0, \beta_1 = 1.0, \delta_1 = 10.0, T_1 = T_2 = 1.0$. For different initial conditions may influence the structure of the attractors of the switched system, all the tests presented in this paper have been done for the initial condition $\mathbb{X}_0 = (-3.7, -3.7, 10.0)$.

In Fig. 3a we present two-parameter bifurcation diagram for parameters $\beta_2 \in [2.3, 18.0]$ and $\delta_2 \in [12.0, 16.0]$ (the rank of the values of $\delta_2$ for which we have detected the existence of symmetric periodic solutions for the studied values of $\beta_2$). In Fig. 3b, c, we show two largest Lyapunov exponent diagrams, one for $\delta_2 = 15.5$, and another one for $\beta_2 = 12.0$. Since a positive value of the maximum Lyaponuv exponent is associated with a chaotic behavior, while the negative is related to stable limit cycles, from the bifurcation diagram Fig. 3a, in conjunction with Fig. 3b, c, the parameter regions $III$, $IV$, $VII$, $VIII$ are the chaotic regions bounded by regular regions $I$, $II$, $V$, $VI$.

The symmetric period 2 solution, shown in Fig. 4a, exists in the region $I$. One can see that the vector fields of the switched system (2.1) may alternate among four stable focuses governed by the two subsystem, respectively, forming the stable symmetric period 2 solution

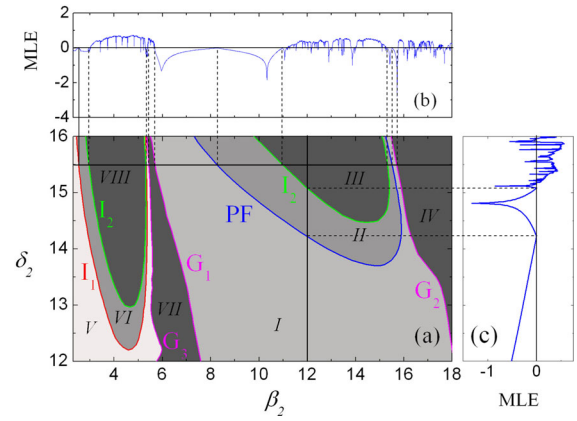


**Fig. 3** **a** Two-parameter bifurcation diagram in the $(\beta_2, \delta_2)$ plane; **b** and **c** the largest Lyapunov exponent for particular values

[24]. With the change of the parameters $\beta_2, \delta_2$, for the symmetric periodic solution, fold and pitchfork bifurcations are possible, as shown in Fig. 3a. Crossing the bifurcation curve of $G_1$ or $G_2$ from the region $I$, the stable symmetric period 2 solution becomes unstable and suddenly change to chaotic oscillation via fold bifurcation. The typical phase portraits are presented in Fig. 4. Crossing the curve of $PF$ from the bottom up, the symmetry of the symmetric period 2 solution will be break, then a pair of stable R-conjugate period 2 solutions (see Fig. 5b) are obtained in region $II$ via pitchfork bifurcation.

With the increase of $\beta_2$, the pair of stable R-conjugate period 2 solutions may undergo pitchfork bifurcation at $PF$, evolving to a symmetric period 2 solution and finally leading to chaos via fold bifurcation at $G_2$. While with the increase in the parameter $\delta_2$, the pair of stable R-conjugate period 2 solutions may become unstable at $I_2$, resulting a pair of R-conjugate period 4 oscillations and finally evolving to chaos via period-doubling bifurcation, respectively. The typical phase portraits are presented in Fig. 5.

In the region $V$, a pair of stable R-conjugate period 1 solutions, shown in Fig. 6a, are obtained. Also, the pair of stable R-conjugate period 1 may undergo fold and period-doubling bifurcation, denoted as $G_3$ and $I_1$ respectively on the bifurcation diagrams in Fig. 3a. Crossing the bifurcation curve of $G_3$ from the left to right, the two R-conjugate period 1 solutions may meet with each other and disappear at $G_3$, leaving the only chaotic solution in the region $VIII$. The typical phase portraits are presented in Fig. 6.

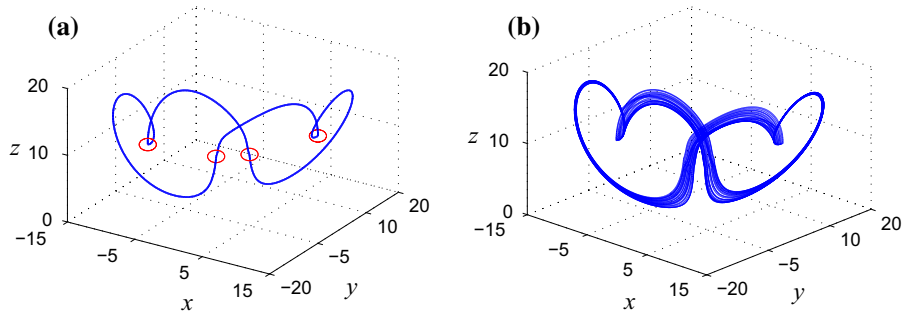


**Fig. 4** A symmetric period 2 solution to chaos for $\delta_2 = 13.5$. **a** $\beta_2 = 7.10$; **b** $\beta_2 = 6.75$

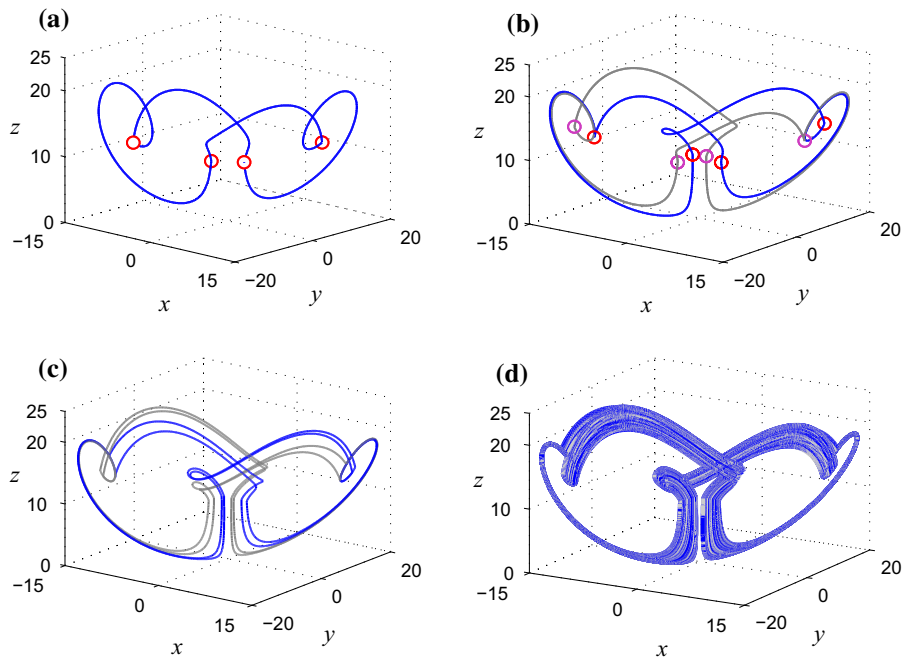


**Fig. 5** A pair of $R$-conjugate period 2 solution to chaos for $\delta_2 = 15.5$, respectively. **a** $\beta_2 = 6.9$; **b** $\beta_2 = 9.6$; **c** $\beta_2 = 11.2$; **d** $\beta_2 = 11.6$

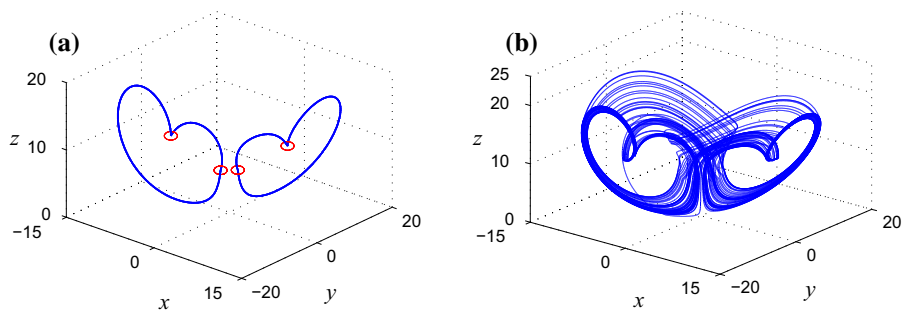


**Fig. 6** A fixed period 1 solution to chaos for $\delta_2 = 13.5$. **a** $\beta_2 = 5.46$; **b** $\beta_2 = 5.72$

Crossing the bifurcation curve of $I_1$ from the bottom up, the two R-conjugate period 1 solutions may become unstable at $I_1$, leading to a pair of stable R-conjugate period 2 solution, while when further crossing the curve of $I_2$ from the bottom up, the two stable R-conjugate period 2 solution change to a pair of stable R-conjugate period 4 solution, and may evolve to chaos, respectively in region $VII$. Finally, the two R-conjugate chaotic solution may expand to interact with each other and disappear, forming an enlarged chaotic solution. The typical phase portraits are presented in Fig. 7.

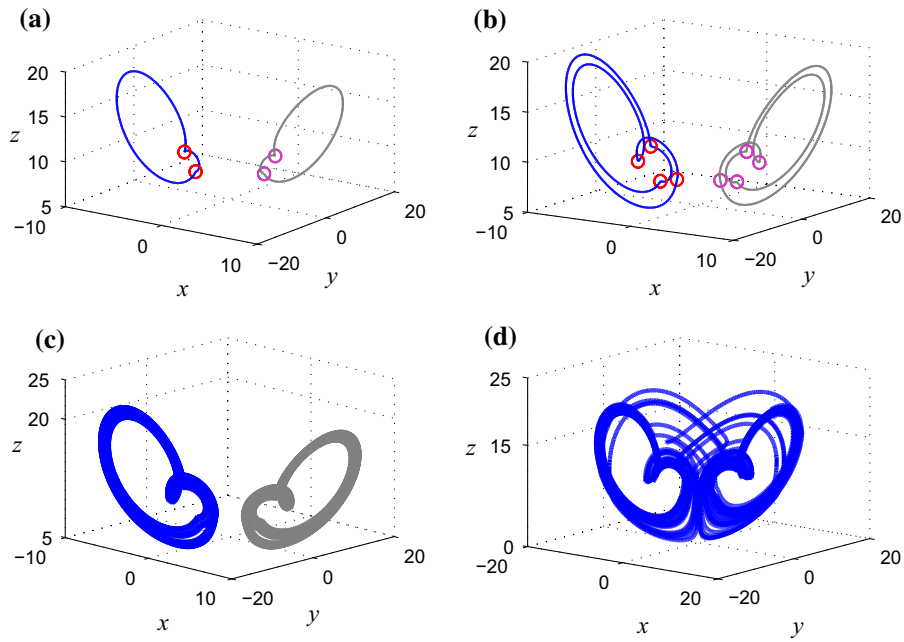


**Fig. 7** A pair of $R$-conjugate period 1 solutions to chaos for $\delta_2 = 14.5$, respectively. **a** $\beta_2 = 2.6$; **b** $\beta_2 = 3.05$; **c** $\beta_2 = 3.4$; **d** $\beta_2 = 4.3$

## 5 Conclusions

Based on the periodic switching scheme, a periodic parameters-switching Lorenz system is established, which may exhibit very complex behaviors such as symmetric and asymmetric periodic oscillations. The trajectory of these solution may be divided into parts governed by the two subsystems respectively, which leading to non-smoothness of the periodic orbits. By introducing the Poincaré map related to all parts of the trajectory, the linearized model of the switched system is constructed. Using bifurcation analysis to the linearized model, two-parameter bifurcation diagrams are obtained, dividing the parameters plane into a set of narrow regions associated with the existence of (symmetric and asymmetric) periodic solutions and chaotic oscillations. We identified basic bifurcation mechanisms leading to transition from regular oscillation to chaos.

There is a question that we are interested in left unsolved in this paper. Is there a curve to distinguish the two R-conjugate chaotic solutions from the enlarged chaotic solutions? This problem seems quite difficult and quite complex. Scientists interested in nonlinear dynamics can pay attention to this problem.

**Acknowledgments** The authors thank the anonymous reviewers for their valuable comments and suggestions that help to improve the presentation of the paper. This work is supported by the National Natural Science Foundation of China (Grant Nos. 21276115, 11272135 and 11202085), the Natural Science Foundation for Colleges and Universities of Jiangsu Province (Grant No. 11KJB130001) and the Research Foundation for Advanced Talents of Jiangsu University (Grant Nos. 11JDG065 and 11JDG075).

## References

1. Lorenz, E.N.: Deterministic non-periodic flow. J. Atmos. Sci. **20**, 130–148 (1963)
2. Khan, M., Shah, T., Mahmood, H., Gondal, M.A., Hussain, I.: A novel technique for the construction of strong S-boxes based on chaotic Lorenz systems. Nonlinear Dyn. **70**, 2303–2311 (2012)
3. Pan, J., Ding, Q., Du, B.X.: A new improved scheme of chaotic masking secure communication based on Lorenz system. Int. J. Bifurc. Chaos **22**, 1250125 (2012)
4. Antonio, A., Fernando, F.S., Manuel, M.: The Lu system is a particular case of the Lorenz system. Phys. Lett. A **377**, 2771–2776 (2013)
5. Schmutz, M., Rueff, M.: Bifurcation schemes of Lorenz model. Phys. D Nonlinear Phenom. **11**, 167–178 (1984)
6. Chua, L.O., Komuro, M., Matsumoto, T.: The double scroll family. IEEE Trans. Circuit Syst. **33**, 1072–1118 (1986)
7. Chen, G.R., Ueta, T.: Yet another chaotic attractor. Int. J. Bifurc. Chaos **9**, 1465–1466 (1999)
8. Liu, C.X., Liu, T., Liu, L., Liu, K.: A new chaotic attractor. Chaos Solitions Fractals **22**, 1031–1038 (2004)
9. Li, R.H., Chen, W.S., Li, S.: Finite-time stabilization for hyper-chaotic Lorenz system families via adaptive control. Appl. Math. Model. **37**, 1966–1972 (2012)

10. Gambino, G., Lombardo, M.C., Sammartino, M.: Global linear feedback control for the generalized Lorenz system. Chaos Solitions Fractals **29**, 829–837 (2006)
11. Farivar, F., Shoorehdeli, M.A., Nekoui, M.A., Teshnehlab, M.: Chaos control and modified projective synchronization of unknown heavy symmetric chaotic gyroscope systems via Gaussian radial basis adaptive backstepping control. Nonlinear Dyn. **67**, 1913–1941 (2012)
12. Ramirez, J.A., Daun, J.S., Puebla, H.: Control of the Lorenz system: destroying the homoclinic orbits. Phys. Lett. A **338**, 128–140 (2005)
13. Gao, T.G., Chen, Z.Q., Gu, Q.L., Yuan, Z.Z.: A new hyperchaos generated from generalized Lorenz system via nonlinear feedback. Chaos Solitions Fractals **35**, 390–397 (2008)
14. Wang, X.Y., Wang, M.J.: A hyperchaos generated from Lorenz system. Phys. A **387**, 3751–3758 (2008)
15. Han, X.J., Jiang, B., Bi, Q.S.: Symmetric bursting of focus-focus type in the controlled Lorenz system with two time scales. Phys. Lett. A **373**, 3643–3649 (2009)
16. Bi, Q.S., Zhang, Z.D.: Bursting phenomena as well as the bifurcation mechanism in controlled Lorenz oscillator with two time scales. Phys. Lett. A **375**, 1183–1190 (2011)
17. Moghtadaei, M., Golpayegani, M.R.H.: Complex dynamic behaviors of the complex Lorenz system. Sci. Iran. **19**, 733–738 (2012)
18. Goebel, R., Sanfelice, R.G., Teel, A.R.: Invariance principles for switching systems via hybrid systems techniques. Syst. Control Lett. **57**, 980–986 (2008)
19. Zhang, C., Yu, Y., Han, X.J., Bi, Q.S.: Dynamical behaviors of a system with switches between the Rössler oscillator and Chua's circuits. Chin. Phys. B **21**, 100501 (2012)
20. Danca, M.F., Tang, W.K.S., Chen, G.R.: A switching scheme for synthesizing attractors of dissipative chaotic systems. Appl. Math. Comput. **201**, 650–667 (2008)
21. Kuznetsov, Y.A.: Element of Applied Bifurcation Theory. Springer, Berlin (1996)
22. Xie, D., Xu, M., Dai, H.H., Dowell, E.H.: Observation and evolution of chaos for a cantilever plate in supersonic flow. J. Fluids Struct. **50**, 271–291 (2014)
23. Xie, D., Xu, M., Dai, H.H., Dowell, E.H.: Proper orthogonal decomposition method for analysis of nonlinear panel flutter with thermal effects in supersonic flow. J. Sound Vib. **337**, 263–283 (2015)
24. Zhang, C., Han, X.J., Bi, Q.S.: Dynamical behaviors of the periodic parameter-switching system. Nonlinear Dyn. **73**, 29–37 (2013)